Journal of Nuclear Materials 407 (2010) 157–164

Contents lists available at ScienceDirect

Journal of Nuclear Materials

journal homepage: www.elsevier.com/locate/jnucmat

A method of examining iron oxides speciation and transport to steam generators during nuclear power reactor startups

Jerzy A. Sawicki [a,*], Barbara D. Sawicka [b], James E. Price [c]

[a] Interatomics, Victoria, British Columbia, Canada V8P 1E3
[b] University of Victoria, Mechanical Engineering, Victoria, British Columbia, Canada V8W 3P6
[c] Ontario Power Generation, Pickering, Ontario, Canada L1V 2R5

ARTICLE INFO

Article history:
Received 13 May 2010
Accepted 29 September 2010

ABSTRACT

Secondary side corrosion products (sludge) collected during one of CANDU1[1] reactor startups from wet layup have been examined by X-ray fluorescence and Mössbauer spectroscopy. The transport and chemical form of iron oxides and oxyhydroxides were determined in condensate, feedwater and preheater outlet as a function of temperature and time. The sludge burst and oxidation states of iron oxides were correlated with the rise of reactor power and corresponding changes in temperature, condensate vacuum and water flow rate. In particular, a sharp γ-FeOOH to Fe_3O_4 switch was observed that coincided in time with the onset of condensate vacuum. Also, it was found that the startup after wet layup is characterized by only brief and fairly small sludge burst at about 30% reactor power and which contributes only a small amount of undesirable α-Fe_2O_3 to total iron transport to steam generator. Thus, sludge burden to steam generators can be minimized with proper layup and startup practices.

1. Introduction

Some amounts of corrosion products (sludge) are always transported by feedwater (FW) to the steam generators (SGs) during reactor steady-state operation [1,2]. However, the bursts of reducible, ferric (Fe^{3+}) oxides such as α-Fe_2O_3, α-FeOOH and γ-FeOOH during reactor startups and transients can be even more degrading [3,4], since sudden delivery to SGs of large amounts of reducible species may result in packing crevices and cavities as well as raise the electrochemical potential over acceptable limits. Such bursts can sometimes be the primary source of fouling and oxidant burden even in units with good operating chemistry practices at steady-state operation [5].

Layup practices during rector shutdowns seem to have decisive effect on the size and oxidation state of startup sludge bursts. Ingress of air, as well as not enough rigorous pH control during shutdowns and layups of secondary cooling systems may result in excessive formation of troublesome ferric (Fe^{3+}) compounds, rather than more acceptable magnetite Fe_3O_4 (Fe^{2+} $Fe_2^{3+}O_4$) in secondary system piping, tanks and other components. During subsequent startups and transients, these species, in the form of sludge bursts, are transported to preheaters and SGs and may result in severe fouling of tubing, packing of crevices, sludge piling and under-deposit corrosion effects. In drastic cases, the total sludge burden and ferric oxides ingress to SGs during startups and transients may be larger than the sludge burden integrated over all period of steady-state operation.

Therefore, there is a considerable interest in understanding and mediating the sludge bursts and undesirable oxidative conditions occurring during reactor startups and transients. Systematic and precise plant data are needed for defining the best procedures on how to avoid excessive sludge transport and minimize the negative effects of oxidized sludge in heaters and SGs. In particular, it is now recognized that better startup oxidant control is needed to minimize the potential for SG tube degradation, especially intergranular corrosion attack and stress corrosion cracking (IGA/SCC) of SG tubes. To define guidelines for oxidant control during shutdown, layup and startup operations, one requires information about a large range of data, in particular: (i) impact of ferric iron species that are formed during plant outages and layups; (ii) oxide reduction measures that can be taken during startups to correct oxidation from earlier steps in the plant history; (iii) rates of oxidation and reduction of deposits as a function of chemistry, temperature, and other parameters during startups; (iv) rates of reduction of oxygen in water as a function of iron oxides inventory, oxygen scavenger type and concentration, temperature, surface-to-volume ratio of pipes and tanks, flow rate, etc., and (v) timing of sludge burst and changes in iron oxide speciation with various operational steps during startups.

In several recent years an extensive work has been performed by us to collect information on the sludge transport and oxidation state in feedwater train during CANDU reactor startups. Sludge properties during startup are affected by both long- and short-term

* Corresponding author.
[1] ™Trademark of Atomic Energy of Canada Limited.

0022-3115/$ - see front matter © 2010 Elsevier B.V. All rights reserved.
doi:10.1016/j.jnucmat.2010.09.056

operational and chemical history of the unit, such as type and duration of outage, type of layup, air exposure, and hydrazine dosage. We have also examined correlations of sludge properties with current procedures of layups and startups. The principal aim of these studies was to collect data that could help to prevent excessive transport of oxidized sludge to the SGs during startups.

The sludge specimens collected during various startups have been analyzed nondestructively using X-ray fluorescence (XRF) and Mössbauer spectroscopy (MS) to determine iron oxides speciation, concentration in water, and in-flow transport rate. As an example of the data that can be obtained and how they can be related to reactor operation, we present here a study of a typical startup conducted after 25 days maintenance outage under wet layup.

2. Operational data

2.1. Plant lay-out

Fig. 1 shows a diagram of a secondary-side water and steam system of the examined 915 MW(e) CANDU reactor. The secondary side of this type of reactor is all-ferrous with stainless-steel condensers and feedwater (FW) heater tubing. The unit has eight recirculating SGs equipped with 4200 alloy I600 (12.7 mm) tubes supported by carbon steel trefoil broach plates and by staggered scallop bar U-bend supports. The system is equipped with full mechanical steam deaerators and FW storage tanks. The pressurized preheaters, where FW is heated by primary coolant, are located outside boilers. This design permits water sampling from both the preheater inlet and outlet, and thus at two distinctly different temperatures, 175 °C and 245 °C at full reactor power, respectively. Henceforth, the preheater outlet will be called PHO. Another point of interest in the system is the condensate extraction pump discharge at ~30 °C, which will be called CEP. The primary temperature of the cold/hot leg is 30 °C/265 °C and the SG operating temperature is 254 °C.

2.2. Water chemistry during steady-state operation

The unit operated at all volatile treatment (AVT) chemistry with pH controlled by 10 mg/kg ammonia from hydrazine breakdown and ~100 ppb hydrazine added between the deaerator and deaerator storage tank. In addition about 7 mg/kg morpholine was added to ensure adequate protection in areas subject to a combination of steam and water. To minimize general corrosion and flow-assisted corrosion of carbon steel and for the I600 tubes protection the pH (as measured at 25 °C) was maintained at least 9.5.

2.3. Sludge sampling

Suspended corrosion products were sampled by filtering water drawn from the condensate extraction pump (CEP); from feedwater (FW) at high-pressure heater outlet and from preheater outlet (PHO) through 0.45 μm pore-sized Millipore acetate membranes. The sampling positions and temperatures there at steady-state operation are shown at the bottom of Fig. 1. At full reactor power, water temperature at the three locations is ~30 °C, 175 °C, and 245 °C, respectively. CEP was sampled locally using a mobile cart and a 6 m line, whereas FW and PHO were sampled in FW sampling room (FWSR) using 100 m and 60 m long sampling lines, respectively. The sampling lines were 9 mm diameter stainless steel butt-welded tubes and the flow through filters was 100 mL/min, with bypass flow up to 200 mL/min. Prior to sampling, FW water and water from PHO were depressurized and cooled down to the temperature of 25–30 °C. Typically, filters were replaced twice daily during startup, and every 6–7 days during steady-state operation. In the examined here startup 70 filters were taken and analyzed.

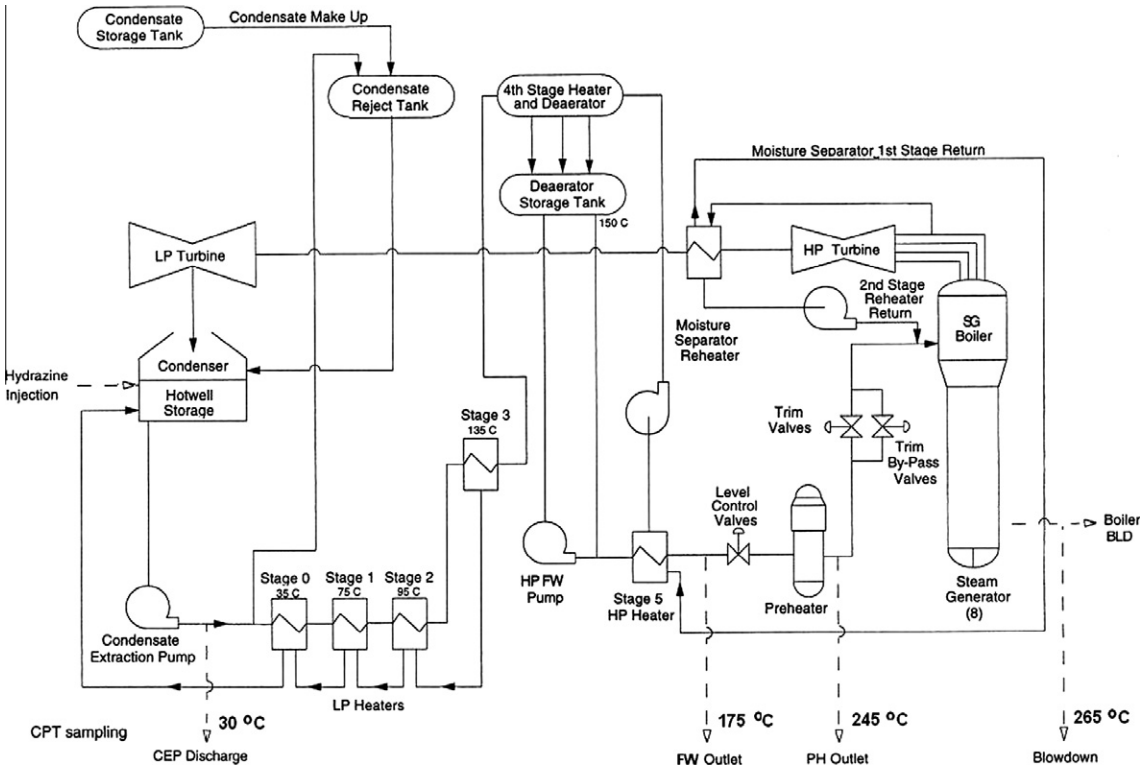

Fig. 1. A diagram of the secondary-side system of examined CANDU reactor.

Our experience is that in properly maintained and flushed sampling system there is not any significant trapping or sludge deposition in sampling lines. Also, cooling the water prior to passing through the membranes is unlikely to change the iron oxide speciation drastically. This is because: (i) there were no signs of blockage noted over many years and startups, (ii) previous testing on the FW sample point showed only minor variations between samples taken locally with mobile sampling cart and remotely in FWSR, and, (iii) for deposits held up in the sample line, only very small and slow changes in oxide concentration and composition are expected, contrary to what is observed during startups. Thus, we can assume that the sludge that is filtered at the sampling stations is dominated by what is transported in the feedwater during the sampling interval.

2.4. Layup operations and conditions

The examined startup was preceded by 25-days-long maintenance layup during which the entire FW system was full of water dosed with hydrazine. With the feedtrain shut down but full, water was drained slowly from the deaerator to the condenser through the boiler feed pump glands, and it was returned once or twice per day from the condenser into the top of the deaerator, and then into the deaerator storage tank, using auxiliary condensate extraction pump. The hydrazine was added directly to the condenser via chemical addition port to specified 35 ppm concentration (it varied between 20 and 50 ppm) in order to maintain pH, provide an excess of hydrazine over dissolved oxygen, minimize corrosion of carbon steel components, as well as to minimize transport of dissolved oxygen to the SGs during early stages of startup when the condenser vacuum is not yet established. During layup period, the pH at CEP gradually decreased from 9.6 to 9.2, and then further to 8.4 – during first 3 days of startup (see Fig. 2). The oxygen concentration at the deaerator outlet was close to saturation (8 ppm), even after a week with hydrazine dosing, because circulation of water through the condensers and deaerator added oxygen faster than the hydrazine could remove it.

2.5. Startup operations

Fig. 2 shows the pH in the condensate, condensate oxygen concentration, PHO (boiler inlet) oxygen concentration and hydrazine concentration at the FW outlet during startup and several days following the startup.

To correlate the observed changes in iron oxides speciation and transport with time it is necessary to describe briefly the timing of subsequent operations during and immediately after the startup. Fig. 3 shows the logs of operational parameters during startup and subsequent normal operation. During the startup discussed in this paper, the reactor power increased from 4% to 40% on day 5, to 60% on day 6, and then continued its slow rise to 90% on day 9.

During a startup, the temperature rises first in the boilers and preheaters because of their contact with the heat-transport system which is heated by decay heat in the core and kinetic heating from the heat-transport pumps, so that during the approach to reactor criticality the preheaters and boilers may be at 85 °C. At this stage the deaerator is heated up electrically. When reactor is critical and ready for heat-up it is brought to stage called zero-power hot (maximum 7% full power) resulting in a normal operating temperature and pressure in the SGs, so that they are capable of producing steam. Steam from the SGs is used in the condenser air extraction system to establish condenser vacuum and to continue heat-up of the deaerator. Steam reject valves open after vacuum is established in the condenser and there is a need to reduce boiler pressure (too much heat in the boilers). The FW outlet temperature depends on the deaerator temperature and whether there is steam for heating on the shell side. The condenser pressure, directly related to the

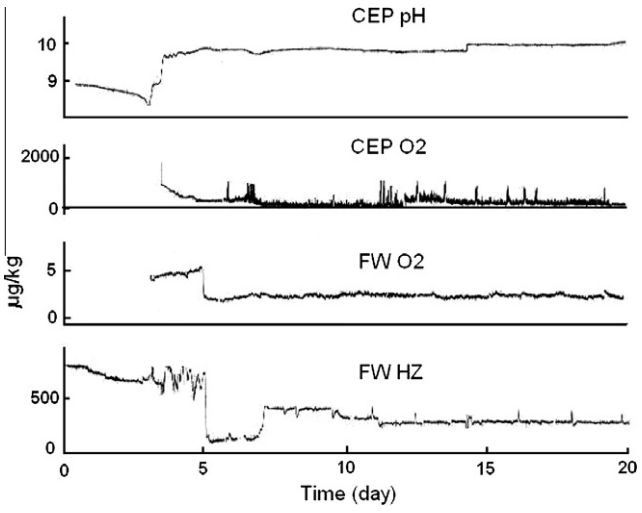

Fig. 2. Chemical parameters presented as a function of time during startup. From top to bottom: condensate pH and oxygen concentration, condensate oxygen, PHO oxygen concentration, and feedwater hydrazine concentration at the FW outlet.

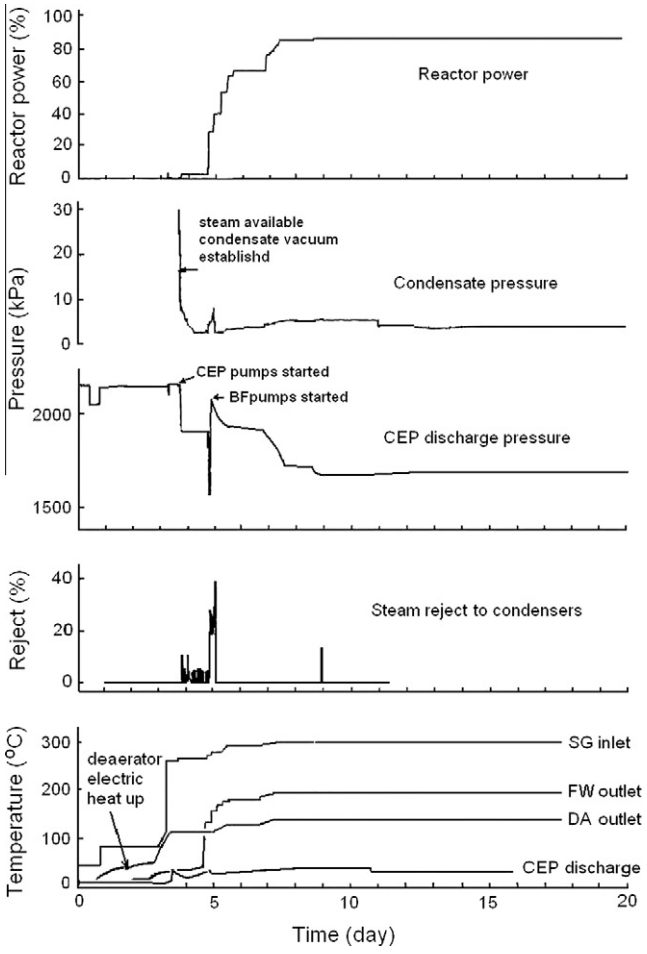

Fig. 3. Operational parameters plotted as a function of time during startup. From top to bottom: reactor power, condenser pressure, CEP discharge pressure, fraction of steam reject to condensers, and the temperatures at condensate discharge, deaerator outlet, FW outlet and SG inlet.

vapor pressure of the water in the condenser, varies with the temperature of cooling water.

Once the physical oxygen control is available, the hydrazine-to-oxygen ratio increases rapidly about 40 times. As far as the oxidant control is concerned, this point represents the transition between wet layup and operation. Reactor is now at zero-power hot, being at full operating temperature and pressure, but still at very low power (<7%). The minimum time at zero-power hot, after a maintenance outage, is 12 h before power is increased. Typical chemical parameters during this stage are listed in Table 1.

At this stage, the sides of the condenser may be at about 50 °C due to direct steam rejection into the condenser, whilst all parts of the system except the moisture separator reheaters are at normal temperature and pressure. A recirculation loop back to one condenser ensures a minimum flow through the condensate pumps with a valve that at low power splits the flow between the feedtrain and the condenser. Flow rate from the condenser to the condensate pumps and back via the recirculation flow does not change. Flow rate up the feedtrain and to the other two condensers does change, as it is due to the steam condensation and it is proportional to the reactor power level.

After completing the required tests, reactor power is increased to about 30% and the turbines are brought on-line. Condensate from the moisture separator reheat system is still returned to the condenser. Reactor power is then increased to 50%, and the water flow from the moisture separators in the first-stage reheat drains is switched from the condenser to the deaerator via the HP heater shell. Reactor power is next increased to 60% and the second-stage reheat flow is switched from the condenser to boiler feed. As reactor power increases further, the flow rate in the piping and across the floor of the condensers further increases. At full reactor power the feedwater flow rate is ~1000 kg/s.

2.6. Analytical techniques

The mass of the sludge collected on the filters during sampling is usually very small, less than 100 μg, which renders their analysis quite difficult. As we have shown, a combination of X-ray fluorescence and Mössbauer spectroscopy methods, as described in detail elsewhere [6,7], provides a more complete analysis and better information on such filtered sludge samples than any other chemical methods. XRF analysis was used primarily to determine the concentration of iron and possible presence of other metals. X-ray fluorescence spectra were obtained using an energy-dispersive X-MET 920 analyzer equipped with 20 mCi ^{109}Cd source emitting 23–25 keV Ag X-rays and a LN_2-cooled Si(Li) detector. A set of reference specimens prepared by vacuum deposition of known quantities of iron oxides on filter membranes was used for calibration of the spectrometer. The iron concentration in water was calculated for each filter using mass of iron as determined by XRF and water flow data recorded during sampling by flow totalizer.

The Mössbauer spectra of 14.4 keV gamma rays in ^{57}Fe were taken using a 15 mCi ^{57}Co source embedded in a 6-μm Rh matrix (Ritverc GmbH). The measurements were performed in transmission geometry. The velocity scale of the spectrometer was calibrated relative to 25 μm α-Fe foil. The temperature during the measurements was stabilized at 295 K. Mössbauer spectroscopy allowed us to determine the speciation of iron oxides and oxyhydroxides, such as magnetite (Fe_3O_4), hematite (α-Fe_2O_3), goethite (α-FeOOH) and lepidocrocite (γ-FeOOH). Ferrihydrite ($Fe_5HO_8{\cdot}4H_2O$), which could be formed by rapid oxidation during shutdown and layup was not observed in any of the specimens. Goethite α-FeOOH was observed in a form of very small nanosized particles and identified only in CEP samples. Metallic iron particles, which occur sometimes in sludges as a product of erosion–corrosion, have not observed in the present study.

It is to be noted that amorphous phases or nanosized particles, such as the goethite observed here, would indicate very large broadening of X-ray diffraction lines and thus cannot be identified by conventional X-ray diffraction analysis, but can be discerned by Mössbauer technique. This represents one of the advantages of using Mössbauer spectroscopy in studies of often poorly crystalline materials, such as are colloidal corrosion products formed through nucleation and precipitation in the reactor water systems. Small particles of this type tend to transform rapidly with changes of water temperature and oxygen concentration. In particular, in regard to absence of goethite in FW and PHO samples, one can refer to the study of thermal topotactic transformation of nanoparticles of α-FeOOH to α-Fe_2O_3 by Christensen et al. [11] using synchrotron radiation X-ray diffraction. For the particles in the size range of 10–100 nm the transformation was observed to start around 170 °C that is at temperature lower than the steady state FW temperature of feedwater of 175 °C. For the goethite particles having average size smaller than 10 nm and in the presence of hydrazine the transformation α-FeOOH to α-Fe_2O_3 can be expected to occur even at lower temperature range.

Table 1
Feedwater operational parameters at zero-power hot.

Parameter	Specification	Desired value			
Action level			1	2	3
Dissolved O_2 (ppb)	<5	ALARA	>5	>25	>75
pH	>9.5	>9.5	<9.5	<8	
Hydrazine (ppb)	>100	>100	<100	>300	

3. Results and discussion

3.1. Iron speciation

In CEP, at the beginning of the startup, the biggest fraction was γ-FeOOH. Fig. 5 shows the correlations observed between the fraction of Fe_3O_4 and fractions of α-FeOOH and γ-FeOOH in CEP and FW sampling positions. The evolution of iron speciation with time during startup is shown in Fig. 4 in % of total iron and in Fig. 6 as iron concentration in μg/kg H_2O (ppb).

The Fe_3O_4 fraction was about 35% on day 0, dropping slowly down to 25% on day 3, and then increasing over the next 2 days to reach the level of 50–60% on day 5 and kept stable at this level thereafter. The fraction of γ-FeOOH was about 50% over day 1, increased slowly to 60% till day 3, and then dropped over the next 2 days down to ~10% Fe, stable at this level during the subsequent steady-state operation. The fraction of α-Fe_2O_3 seems to stay close to an average value of 12–15% throughout the whole period of 20 days. The short-term switch from the dominant γ-FeOOH to the dominant Fe_3O_4 that occurs at day 3 might be related to low CEP pH at this time. The second (prominent and permanent) switch from γ-FeOOH to Fe_3O_4 that starts at day 4 seems to be caused by establishing of the condenser vacuum, accompanying sudden drop in the oxygen content and the resultant electrochemical potential, that occurs in the condensate in the middle of day 3. It is also interesting to observe that until day 6, the changes in α-FeOOH and γ-FeOOH percentages with time tend to mirror each other; whereas after day 7 the similar mirroring effect can be seen for α-FeOOH and Fe_3O_4, see top diagram in Fig. 4. It is also worth noting that approximately after 1 week from the beginning of the startup the fractions of Fe in four oxides returned to their pre-shutdown values.

In FW, the fraction of γ-FeOOH is dominant at day 0, similar to CEP, increasing slowly from 55% to 65% during the first 4 days, and then decreasing sharply over day 5 to ~20% Fe. Fraction of Fe_3O_4 is

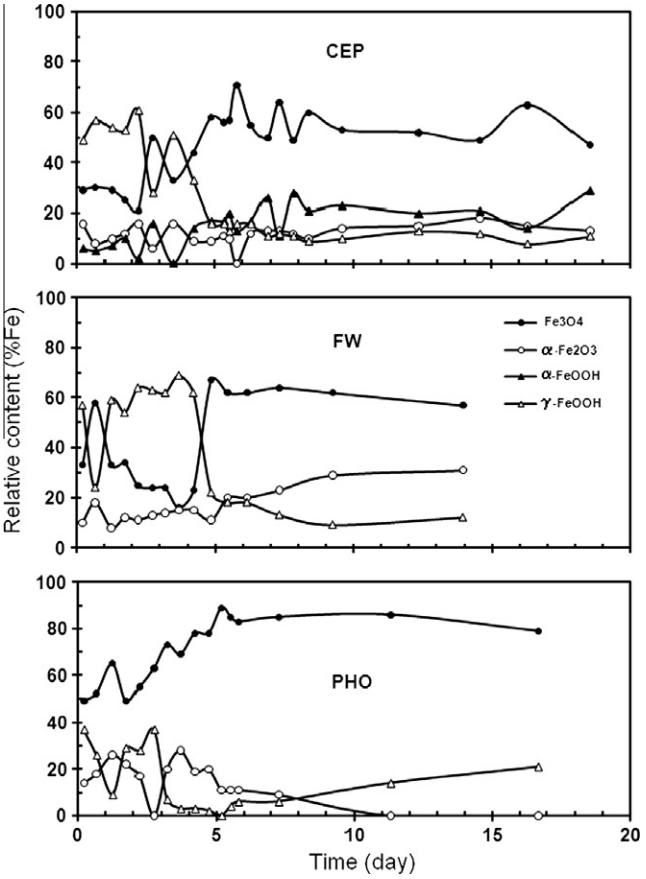

Fig. 4. Iron speciation data for sludge collected at CEP, FW and PHO locations presented as a function of time during reactor startup.

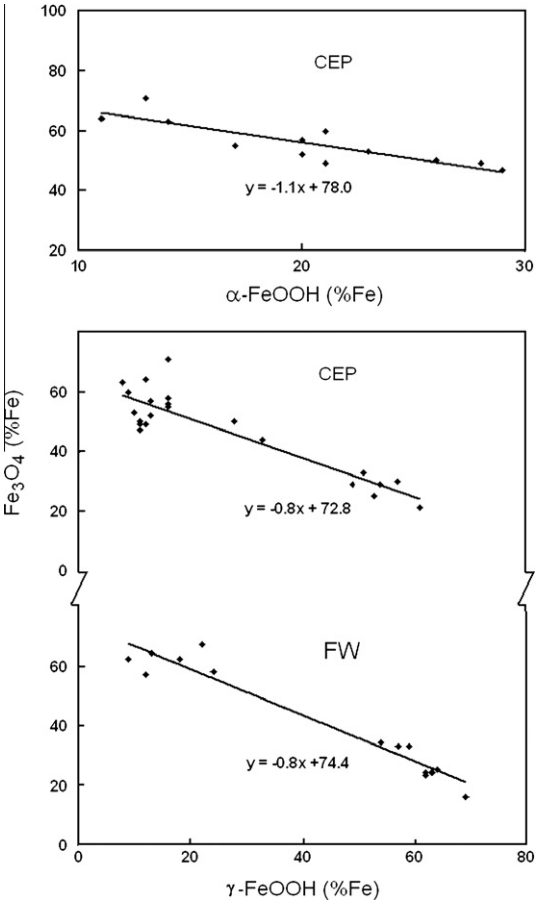

Fig. 5. Observed correlations between the fraction of Fe_3O_4 and fractions of α-FeOOH and γ-FeOOH in CEP and FW sampling positions.

~30% at day 0, dropping slowly over the first 5 days to ~20% Fe, and then increasing sharply at day 5 to ~60% to remain at this level. Change in the Fe_3O_4 fraction over the first 5–6 days is almost exactly opposite to the changes in the γ-FeOOH fraction, see Fig. 4. The switch from γ-FeOOH-to- Fe_3O_4 seems to occur in FW about one half-day later than it does in CEP. The balance of iron in FW is in form of α-Fe_2O_3, which fraction increases steadily from about 10% at day 0 to ~30% after 10 days.

In PHO, the Fe_3O_4 fraction is dominant over the whole startup period, increasing steadily from 50% on day 0 to ~80% on day 6. Thus, the Fe_3O_4 fraction during steady-state operation was higher in PHO (~50% Fe) than in CEP and FW (~60%). This can be explained by higher temperature at PHO and resulting low concentration of dissolved oxygen. The γ-FeOOH fraction in PHO was ~40% on day 0, decreased to 10% in day 1, then increased to 40% over the next 2 days, dropped down sharply to under 5% on day 3, and remained there for several days, to start rising on day 7 to reach ~20% on day 17. The balance of iron in PHO is in the form of α-Fe_2O_3; it goes down with time starting from day 3 to 4 until it becomes negligible during steady-state operation. Another interesting effect is the steady increase in γ-FeOOH fraction at the PHO that starts in day 7 and by day 17 reaches about 20%. This could be caused by production of γ-FeOOH in the condenser and lack of time to convert it due to low residence time of sludge in feedtrain at high power.

3.2. Iron concentration in water

The MS and XRF analyses data were used to determine mass concentrations of various iron oxides. Fig. 6 (top) shows the mass

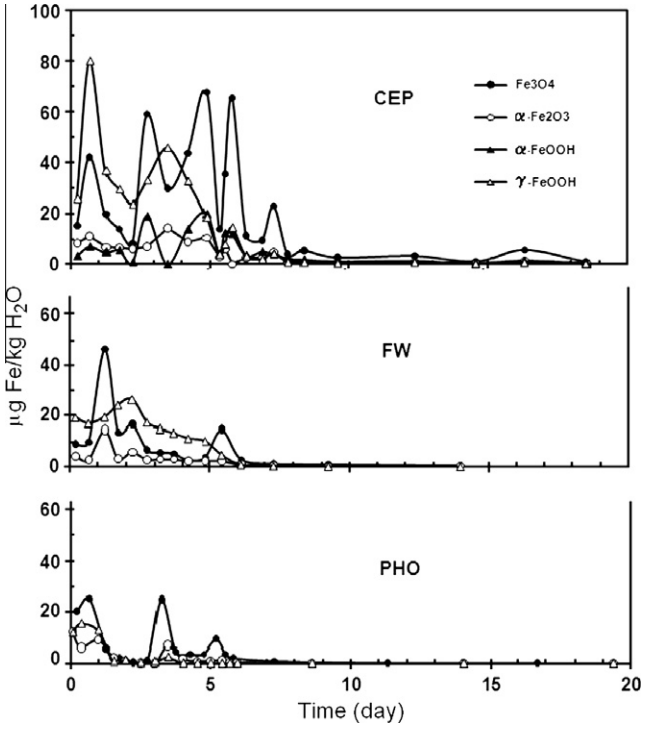

Fig. 6. Concentration of iron oxides in water for specimens collected at CEP, FW and PHO locations presented as a function of time during reactor startup.

concentrations, in μg Fe/kg H_2O, i.e., ppb, as a function of time in three sampling locations. In general, iron concentrations in FW and PHO were smaller than in CEP, and diminished from their starting values of ~80 ppb at FW and ~50 ppb at PHO, slowly in FW, and much faster in PHO, and after day 8 they stabilized below 1 ppb in both positions. Iron concentration in CEP shows a more complex behavior that reflects primarily the timing and complexity of streams fed back to condensers during startup. In day 1, the Fe concentration was up to 140 ppb, then it decreased in day 2 to 40 ppb, increased during days 3–5 to 100–120 ppb range, peaked again in day 6, decreased slowly through next 3 days to ~20 ppb, and after day 8 stabilized below 10 ppb. The peaks of iron concentration by the end of day 5, during day 6, and after day 7 coincide with subsequent reactor power increases. The peak of iron by the end of day 5 also coincides with large reject fraction of steam to condensers from boilers at this time.

3.3. Sludge transport

The sludge mass transport as a function of time was calculated in three sampling locations assuming that the water flow rate is proportional to the reactor power, and that the flow at full reactor power is 1000 kg/s. To account for the mass of oxygen in oxides the mass of iron measured by XRF was multiplied by a factor of 1.3. Bottom panel in Fig. 7 presents total sludge transport in CEP, FW and PHO locations as a function of time during reactor startup. The sludge transport at CEP outlet is below 1 mg/s during the first several days, it rises sharply to 60 mg/s (5 kg/day) during day 4, drops down to 15 mg/s and peaks again in day 6, drops down again and peaks up to 30 mg/s in day 7 to decline to on average 4 mg/s during normal operation. Sludge transport measured at FW and PHO shows only a very short burst by the end of day 5, to a value of ~10 mg/s (0.9 kg/day) and 6 mg/s (0.5 kg/day), respectively. Numerical characteristics of the startup sludge burst are summarized in Table 2. The time-integrated masses of sludge transported through CEP, FW and PHO during days 2 through 9 were 10 kg, 0.5 kg and 0.2 kg, respectively. Thus, the sludge transport to SGs during investigated startup compares very favorably with annual sludge burden for this unit, which at 2 ppb Fe steady-state full reactor power value is estimated to be close to 100 kg [1].

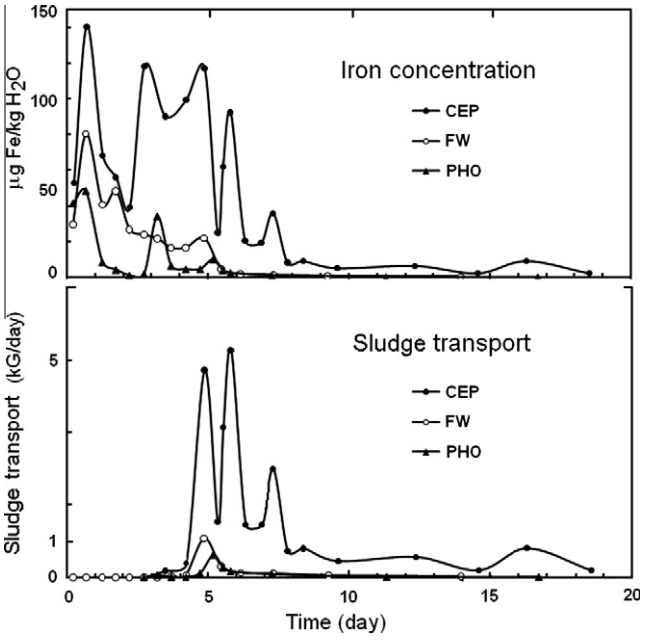

Fig. 7. Iron concentration in water and sludge transport in CEP, FW and PHO locations as a function of time during reactor startup.

Table 2
Sludge transport and reactor power during startup.

Sludge transport (mg/s)	Day 2	Day 5	Day 6	Day 9
CEP	<2	40–60	30–15	4
FW (HX5)	<1	10	3	1
PHO	0	6	0.5	0.2
Reactor power (%)	0–4	4–70	70	90

The observed sludge bursts correlate with the rate of the reactor power increases, and correlate with the corresponding changes in temperature and flow rate, rather than with the reactor power itself. The first high sludge burst, up to 60 mg/s, is observed during the initial sharp power increase from 4% to 30%, accompanied by bringing turbines into service to 70%. Over the subsequent 2 days, with the reactor stable operation at ~70% power, the sludge transport is low. The second sludge burst, up to 30 mg/s, occurs on day 7, when the reactor power increases from 70% to 90%.

4. Correlation of sludge properties with operational parameters

Sludge composition and transport in various locations along feedtrain during startup can be affected by a number of phenomena and influenced by various operating parameters. In particular, (i) wet and dry layup, as well as past history of the unit, may result in drastically different sludge properties; (ii) the composition of sludge produced in the condenser could change once the condenser vacuum is established; (iii) the phase composition of sludge existing in the condenser could change once steam is produced; (iv) deaerator storage tank removes a lot of sludge transported from the condenser, and the fraction removed will depend on such factors as its size and morphology, which could be phase dependent; and (v) hydrazine concentration and temperature are higher downstream of the storage tank, which might affect phase composition of samples at FW and PHO. We will discuss these various factors below in view of the experimental results of this work.

The iron oxidation type and sludge transport is certainly related to the type of outage. The examined startup was preceded by a fairly short 25 day outage, during which the feedtrain was kept under wet layup. Typically, the sludge burst is small and brief under these conditions. Startups from wet layups usually result in much less sludge transport to the SGs than startups from dry layups, and therefore should be considered preferable.

One factor to consider is the presence and speciation of deposits in various form and quantity on all steel surfaces in the system. Such deposits, when exposed to water and steam flows – especially during startup transients – can be entrained and may represent a large fraction of the total transported material. Condenser floor deposits are especially abundant and may strongly contribute to the startup sludge bursts. Examination of condenser floor deposits from other units indicates that the floor deposits tend to be mixed α-Fe_2O_3, γ-FeOOH, and Fe_3O_4 [8]. Between the CEP and the deaerator, the deposits are loose and flaky, with iron present as a mixture of various oxides. Between the deaerator storage tank and the inlet of the high-pressure heater (FW), the piping is covered with a tight and adherent layer of α-Fe_2O_3. Further upstream piping and the preheater are covered with a tight and adherent layer of Fe_3O_4. This coverage might have an influence on what type of oxide would be most easily transported.

Generally, the phase composition of transported sludge can change due to release or removal of the oxide coating from piping or the transformation between iron oxides, or the combination of the two. In particular, an increase in sludge transport due to two-phase flow in the steam lines between the SG and the condenser would cause some flow-assisted corrosion (FAC) and

release of oxide coatings from piping which previously had been identified as Fe_3O_4. This effect, however, cannot be predominant, because there is no evidence of any sludge carried out in the steam, and the switch occurs at low reactor power when the flow rates are low.

The degree of conversion of potential oxidants α-FeOOH, γ-FeOOH and α-Fe_2O_3 to desirable Fe_3O_4 has corrosion implications for the boiler tubes, and it is very important to know more about the nature, rate, timing and location of this transformation in the system during startups. During the examined startup, we observed a decrease in the γ-FeOOH fraction with a simultaneous increase in the Fe_3O_4 fraction. The timing of this switch is different in different parts of the system, and is consistent with the interpretation that the transformation is the result of a vacuum/steam effect in CEP, and temperature effects in FW and PHO. The observed γ-FeOOH-to-Fe_3O_4 switch occurs at different times in the three sampling locations, but always before the beginning of the sludge burst and at a low water flow rate. The observed transition from γ-FeOOH to Fe_3O_4 can be the result of the transformation between the two iron compounds. The possibility of this effect is supported by the mass balance of different sludge fractions and timing of this transition: (i) in all three locations, an increase in the Fe_3O_4 fraction is always accompanied by a simultaneous and equal in magnitude decrease in the γ-FeOOH fraction, while the fractions of α-Fe_2O_3 and α-FeOOH remain virtually unchanged (Fig. 4), (ii) the total iron transport is steady during the time periods when the switch between phases occur (Fig. 6), and (iii) laboratory tests [10] show that γ-FeOOH formation is favored by high oxidation potential and Fe_3O_4 formation is favored by low oxidation potential. Consequently, assuming that our interpretation is correct, what is predominantly transported to the steam SGs depends on whether the γ-FeOOH to Fe_3O_4 switch was completed or not before the sludge burst.

At the beginning of the startup cycle, iron was found predominantly in the form of γ-FeOOH, whereas later it was mostly Fe_3O_4. A sudden switch from γ-FeOOH to Fe_3O_4 in the CEP coincided with establishing the condenser vacuum (steam availability) while reactor power was still below ~30% and before the sludge burst. In the PHO and FW, the transition is thought to be caused by a temperature effect, and it occurs in the PHO earlier and in FW somewhat later, than the transition in the CEP. The observed γ-FeOOH-to-Fe_3O_4 switch is thought to be caused by transformation between the two oxides. This interpretation is supported by the observations, that the total iron transport is steady during the switch, and that an increase in the Fe_3O_4 fraction is accompanied by a simultaneous and equal in magnitude decrease in the γ-FeOOH. The switch occurs at different times in the three locations, but always during a low flow rate and before the beginning of the sludge burst.

The observed differences in timing of γ-FeOOH decrease along the feedtrain can be correlated with operational conditions during startup. The large decrease of γ-FeOOH in condensate coincides with the establishing of condenser vacuum. At this time there is typically still a large amount of hydrazine in the water, vacuum lowers the oxygen concentration and steam increases the temperature. The net result is the establishment of reducing conditions which favor a more reduced oxide. In the feedwater although there is still lot of hydrazine there may also be enough oxygen to prevent full reducing conditions. The reduction of γ-FeOOH in the feedwater coincides not only with the increase in temperature but the drop in oxygen seen in Fig. 2. The ratio of hydrazine to oxygen may be the key since Fig. 2 shows FW N_2H_4 in the μg/kg range while the condenser is likely at mg/kg. In summary the change at all three points may be due to establishing reducing conditions by increasing the hydrazine/oxygen ratio by physical removal on one hand and chemical removal on the other.

It is possible that the cause of this effect is different in CEP than in FW and PHO. In CEP, the transition is gradual and occurs during day 4 at very low reactor power. It coincides with the start of steam rejection to condensers, and thus with establishing of condenser vacuum. We suggest that when steam is routed to the CEP, iron is transformed into its reduced state. At FW and PHO, the γ-FeOOH-to-Fe_3O_4 switch coincides with the temperature rising above a threshold value (Fig. 2) occurring at the PHO much earlier, and at FW somewhat later, than the transition in the CEP. Whereas the FW temperature does not increase until steam is produced in the boilers, the PHO temperature increases in response to the increased heat-transport temperature. At FW, the switch is sharp, and occurs on day 5, when the temperature reaches about 140 °C. At the PHO a sharp decrease in the γ-FeOOH fraction is noticed already during day 3, when the temperature at the SG inlet reaches 255 °C. The interpretation of the FW and PHO transitions as a temperature effect agrees with the observation that because the temperature is higher at the PHO than at FW, the observed steady-state fraction of Fe_3O_4 is higher at PHO.

It should be noted here that the similar sudden switch between and γ-FeOOH fractions has been as well observed in the tests in a dedicated loop experiments at Studsvik Nuclear in Sweden, in conditions simulating condensate and feedwater in CANDU and PWR reactors [9]. In these tests it was found that the fraction of Fe_3O_4 in the condensate decreased from about 55% to about 5% when increasing the oxygen level from 5 ppb to 50 ppb at 100 ppb hydrazine.

Contrary to the behavior of γ-FeOOH during examined startup, the α-Fe_2O_3 was found to be a rather stable fraction. Some fluctuations in the α-Fe_2O_3 contents were observed in PHO; however, no dramatic change was observed. Our present results indicate that the α-Fe_2O_3 formed in the feedtrain is transported to the SGs. The inability to considerably alter the α-Fe_2O_3 fraction in the feedtrain may mean that further steps need to be taken to limit the sludge transport during startups, instead of trying to chemically make the oxides more acceptable.

The concentration of iron during startup was significantly lower in preheater outlet than in preheater inlet, which indicates that most of the sludge was not transported to the SG, but that it was deposited in the preheater. During the sludge burst as well during steady state reactor operation iron occurred mainly as Fe_3O_4. The sludge transport during the reactor steady-state operation following startup decreased to very low levels. There appears to be no clear relationship between the phase of the deposits and the amount formed. We have seen large sludge bursts previously that have had very high γ-FeOOH fractions.

We observed that sludge bursts correlate with the rate of increase of reactor power. Large burst was observed at the initial reactor power increase (5–30%), and especially when the turbine was brought on-line, and smaller burst was observed at the later power increase (70–90%). This may indicate a finite source of sludge that are mobilized by the initial increase in-flow; further increases in-flow do not have the same impact, since a relatively small amount of sludge remains to be entrained by the higher flow.

Another factor to consider is the hydrazine and oxygen concentrations during outages. During the unit wet layup, the fully oxygenated water is being dosed with hydrazine. The hydrazine may have impeded corrosion by acting as a base or by working to limit the oxygen concentration (electrochemical potential) at the metal surface; the hydrazine will also react directly with oxygen.

At low reactor powers, there would be a relatively long residence time in the feedtrain. This may explain the observed drop in iron transport between the condensate and the high-pressure heater. The drop in iron transport between the high-pressure heater and outlet could also be due to plating out on piping or in the preheater itself, with a temperature-dependent rate of attachment.

Chemical conditions during the outage, as well as during previous outages, are thought to be largely responsible for the differences seen in sludge form and transport during startups. In particular, during startup of a similar unit after prolonged dry layup (with moist air) a much larger amount of α-Fe_2O_3 entered to SGs than after wet layup described here. This suggests that dry layups of feedtrain should be avoided or better controlled.

5. Summary and conclusions

The application of X-ray fluorescence and Mössbauer techniques proved to be useful in studying characteristics of sludge bursts during power reactor startups. Data on sludge transport and the iron oxidation state were obtained for one of CANDU reactor startups after a short maintenance outage under wet layup, with the feedwater system full of water and dosed with hydrazine. Such conditions of layup were found to inhibit corrosion processes and diminish sludge transport during subsequent reactor startup and steady-state operation.

The transport of reducible iron oxides and oxyhydroxides; hematite α-Fe_2O_3, goethite α-FeOOH and lepidocrocite γ-FeOOH, and the rate at which the fraction of magnetite Fe_3O_4 in feedwater increases during startup, were determined in condensate, feedwater and preheater outlet as a function of temperature and time, and correlated with the changing chemistry and operational parameters.

The examined startup was characterized by only small and brief sludge bursts, a fairly small α-Fe_2O_3 fraction, and small iron transport to SGs mostly in a form of Fe_3O_4. Timing of burst was found to correlate with the rate of reactor power increase, and with the changes in the temperature and flow rate. A larger burst was observed at the initial reactor power increase, and coincided with the timing of the turbine brought on-line. A second, smaller burst was observed at the final power increase that brought reactor to its steady operation at full power. This indicates that the sludge is mobilized primarily by increasing water and steam flows. A pronounced and fast γ-FeOOH-to-Fe_3O_4 switch was also observed, and it coincided with establishing the condensate vacuum.

The information obtained can be used to improve the chemistry control of secondary water systems in pressurized nuclear power reactors, and especially to minimize negative effects of excessive sludge formation, transport and fouling of SGs with undesirable ferric iron oxides, as the result of improper shutdown, layup and startup operations. The characteristics of the sludge bursts in PWRs should not much differ from observed in CANDU plants, but ought to be examined in view of differences in the design of the secondary systems, water chemistry and operational procedures.

Acknowledgements

The Mössbauer and XRF analyses described in this paper were performed at AECL Chalk River Laboratories and were funded by the CANDU Owners Group R&D Program, Chemistry Components and Materials Working Party. The authors thank Dr. R.L. Tapping (AECL), Dr. M. Brett (OPG) and colleagues associated with AECL, Ontario Power Generation, Studsvik Nuclear and Electric Power Research Institute for helpful discussions and comments.

References

[1] J.A. Sawicki, M.E. Brett, R.L. Tapping, Corrosion product transport, oxidation state and remedial measures, in: Proc. Third Intern. Conf. on Steam Generators and Heat Exchangers, Toronto, Canadian Nuclear Society, June 1998, pp. 465–479.
[2] M.E. Brett, A.P. Quinan, J.E. Price, J.A. Sawicki, Secondary side electrochemical potential monitoring and the redox state of corrosion products in ontario hydro nuclear, in: Proc. Seventh Intern. Conf. on Water Chemistry of Nuclear Reactor Systems, vol. 1, Bournemouth, October 1996, pp. 407–414.
[3] Proc. EPRI Workshop on Startup Oxidant Control, Chattanooga, EPRI TR-112815, January 1999.
[4] Proc. COG Workshop on Layup, shutdown and startup chemistry optimization, Toronto, in: J.A. Sawicki (Ed.). COG 99-66-I, 2–3 March 1999.
[5] B.D. Sawicka, J.A. Sawicki, J.E. Price, Sludge oxidation and transport during startups, in: Proc. 2001 PWR/BWR Plant Chemistry Meeting, San Antonio, EPRI, 2001.1001489, January 2001.
[6] J.A. Sawicki, A. Molander, A. Stutzmann, Precipitation and transformation of iron species in the presence of oxygen and hydrazine in a simulated stainless steel feed water system, in: S. Ritter, A. Molander (Eds.), Corrosion Monitoring in Nuclear Power Systems: Research and Applications, Chapter 14, European Federation of Corrosion, Manley Publishing ISBN-13, 978-1-906540-98-2, 2010, pp. 221–238.
[7] B.D. Sawicka, J.A. Sawicki, Corrosion-product transport analysis by nondestructive X-ray and gamma-ray methods, in: Proc. Intern. Water Conf., Pittsburgh, October 1999.
[8] J.A. Sawicki, J. Price, M.E. Brett, Corrosion product inventory: the bruce-b secondary system, in: Proc. Third International Conference on CANDU Maintenance, Toronto, Canadian Nuclear Society, November 1995, pp. 53–56.
[9] S. Forsberg, J.A. Sawicki, P.-O. Andersson, A. Molander, Studies of iron redox states, corrosion potentials and oxygen reduction in a simulated feedwater train, in: Proc. Steam Generator Secondary Side Management Conf., Savannah, Georgia, February 2003.
[10] C.U. Schwertmann, R.M. Cornell, Iron Oxides in the Laboratory, VCH Publishers, Inc., New York, 1991.
[11] A.N. Christensen, T.R. Jensen, C.R.H. Bahl, E. DiMasi, J. Solid State Chem. 180 (2007) 1431.